

1 New insights on lake sediment DNA from the catchment: importance of taphonomic and analytical  
2 issues on the record quality

3

4 Giguet-Covex C.<sup>1,2</sup>, Ficetola G.F.<sup>3,4</sup>, Walsh K.<sup>1</sup>, Poulenard J.<sup>2</sup>, Bajard M.<sup>2</sup>, Fouinat L.<sup>2</sup>, Sabatier  
5 P.<sup>2</sup>, Gielly L.<sup>3</sup>, Messenger E.<sup>2</sup>, Develle A.L.<sup>2</sup>, David F.<sup>5</sup>, Taberlet P.<sup>3</sup>, Brisset E.<sup>6,7,8</sup>, Guiter F.<sup>6</sup>,  
6 Sinet R.<sup>6</sup>, Arnaud F.<sup>2</sup>

7

8 1- BioArch-Department of Archaeology, University of York, YO10 5DD, UK

9 2- EDYTEM, UMR 5204 CNRS, Univ. Savoie Mont Blanc, Pôle Montagne, 73376 Le  
10 Bourget du Lac, France

11 3- Univ. Grenoble Alpes, Univ. Savoie Mont Blanc, CNRS, LECA, 38000 Grenoble,  
12 France

13 4- Department of Environmental Science and Policy, Università degli Studi di Milano.  
14 Via Celoria 26, 20133 Milano, Italy

15 5- CEREGE, UMR CNRS 7330, IRD 161-Marseille Université, Technopôle de  
16 l'Arbois Méditerranée, BP 80, 13545 Aix en Provence cedex 4, France

17 6- Aix-Marseille Univ, Avignon Univ, CNRS, IRD, IMBE. Aix-en-Provence, France

18 7- Institut Català de Paleoecologia Humana i Evolució Social (IPHES). Tarragona,  
19 Spain

20 8- Àrea de Prehistòria, Universitat Rovira i Virgili. Tarragona, Spain

## 21 **Supplementary materials**

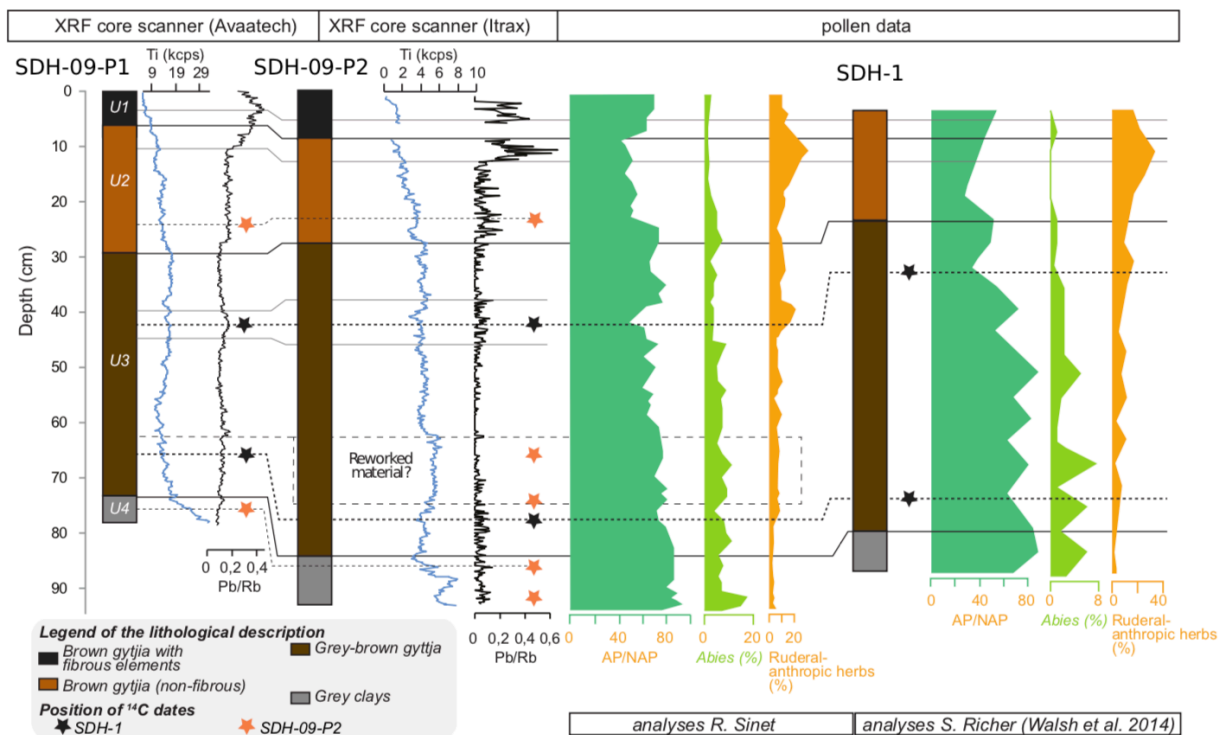
### 22 **1. Sediment lithology and dating**

#### 23 **1.1. Lake Serre de L'Homme**

24 Three cores from Lake Serre de l'Homme (SDH-1, SDH-09-P1, SDH-09-P2) were included in our  
25 study in order to provide an age-depth model and determine the sedimentation rate on the core we  
26 used for DNA analyses (SDH-09-P1). These sediment cores are characterised by four different  
27 units (Supplementary figure 1). Unit 1 (U1) is made of brown fibrous gyttja sediments with an  
28 organic matter content around 50-60% according to the loss on ignition at 550°C (LOI 550°C).  
29 Unit 2 (U2) is made of a brown non-fibrous gyttja with an organic matter content varying between  
30 30 and 50%. The organic matter content varies around 30% in unit 3 (U3). The gyttja sediments  
31 from this unit are grey-brown. In unit 4 (U4), sediments have lower content in organic matter and

32 are mostly made of grey clays. Two  $^{14}\text{C}$  dates were available on cores SDH-1 and five on core  
 33 SDH-09-P2 (see Supplementary table 1). Arboreal pollen/non-arboreal pollen ratio, *Abies* signal  
 34 and the ruderal-anthropic herbs signal were used to project the position of the two  $^{14}\text{C}$  dates from  
 35 the core SDH-1 on the core SDH-09-P2 (Supplementary figure 1 and table 1). Pollen on core SDH-  
 36 1 (taken in 2006 with a Russian corer close to the shoreline) was analysed by S. Richer (IMBE,  
 37 Université Aix-Marseille) and published in (Walsh et al., 2014). Pollen on core SDH-09-P2 (taken  
 38 in the centre of the lake in 2009 with a UWITEC coring device) was analysed by R. Sinet (IMBE,  
 39 Université Aix-Marseille). Positions of dates were also projected on core SDH-09-P1 based on the  
 40 lithological descriptions and geochemical signals (titanium and lead/rubidium ratio) from the XRF  
 41 core scanner analyses (Supplementary figure 1). SDH-09-P1 was analysed at EDYTEM  
 42 (Université Savoie-Mont Blanc) using an XRF core scanner Avaatech (X-Ray beam generated  
 43 with a rhodium anode and a 125  $\mu\text{m}$  Beryllium window) with the following settings: run 1 at 10  
 44 kV, 1.2 mA, a counting time of 20 s and a resolution of 2 mm; run 2 at 30 kV, 0.75 mA, a counting  
 45 time of 60 s and a resolution of 2 mm. SDH-09-P2 was analysed at CEREGE (Université Aix-  
 46 Marseille) with a Cox Analytics *Itrax* core scanner <sup>1</sup>. The X-Ray beam was generated by a 3kW  
 47 molybdenum tube, and the following settings were applied: 30kV, 30mA, a counting time of 20 s  
 48 and a resolution of 2 mm.

49



50  
 51 **Supplementary figure 1. Lithological descriptions and correlations for cores taken from Lake Serre de**  
 52 **l'Homme. Core correlations are based on titanium and lead/rubidium ratio measured by XRF core scanner for cores**

53 SDH-09-P1 and P2, while SDH-09-P2 and SDH-1 were correlated using pollen analyses (arboreal pollen/non-arboreal  
 54 pollen ratio, *Abies* and anthropogenic indicators).

55  
 56 Two <sup>14</sup>C dates from the core SDH-09-P2 were too old to respect the stratigraphic principle of  
 57 superposition (Supplementary figure 2A). They were thus removed to generate the age-depth  
 58 model on core SDH-09-P2. Moreover, based on the presence of these two dates from reworked  
 59 materials and the enrichment in titanium only recorded in SDH-09-P2, we propose the presence of  
 60 a reworked sediment deposit (or of an erosive event which mobilised old plant remains buried in  
 61 soils) in the core SDH-09-P2 (Supplementary figures 1 and 2A). However, whether this deposit  
 62 corresponds to reworked materials or not has no consequences for our study. For the recent period,  
 63 two supplementary chronological points corresponding to recent atmospheric lead pollutions and  
 64 highlighted by high Pb/Rb ratio were included to generate the age-depth model. The lead/rubidium  
 65 ratio was used to highlight these lead pollution phases because it permits a correction from the  
 66 enrichment effect triggered by bedrock erosion. In fact, rubidium represents a purely lithogenic  
 67 element and is not affected by weathering or diagenesis processes. The upper lead peak, only  
 68 recorded at 2.5 cm in the core SDH-09-P1 because of a gap in measurements on core SDH-09-P2,  
 69 is attributed to the effects of the oil crisis in 1973-74 and the introduction of unleaded gasoline in  
 70 1985 <sup>2,3</sup>. We thus proposed 1979  $\pm$  6 AD as a date for this stratigraphic marker. Below this peak,  
 71 the strong increase of Pb/Rb (at 12,5 cm for SDH-09-P2 and at 10 cm for SDH-09-P1) is attributed  
 72 to the pollution triggered by the Second Industrial Revolution at the beginning of the 20<sup>th</sup> century  
 73 and the introduction of leaded gasoline in the 1920s <sup>2,3</sup>. An age of 1920  $\pm$  20 AD was proposed for  
 74 this increase in Pb/Rb. The age-depth models of the two cores were generated using the *R software*  
 75 and the *R-code package 'Clam' version 2.2* <sup>4</sup>. Models with linear interpolations were selected.

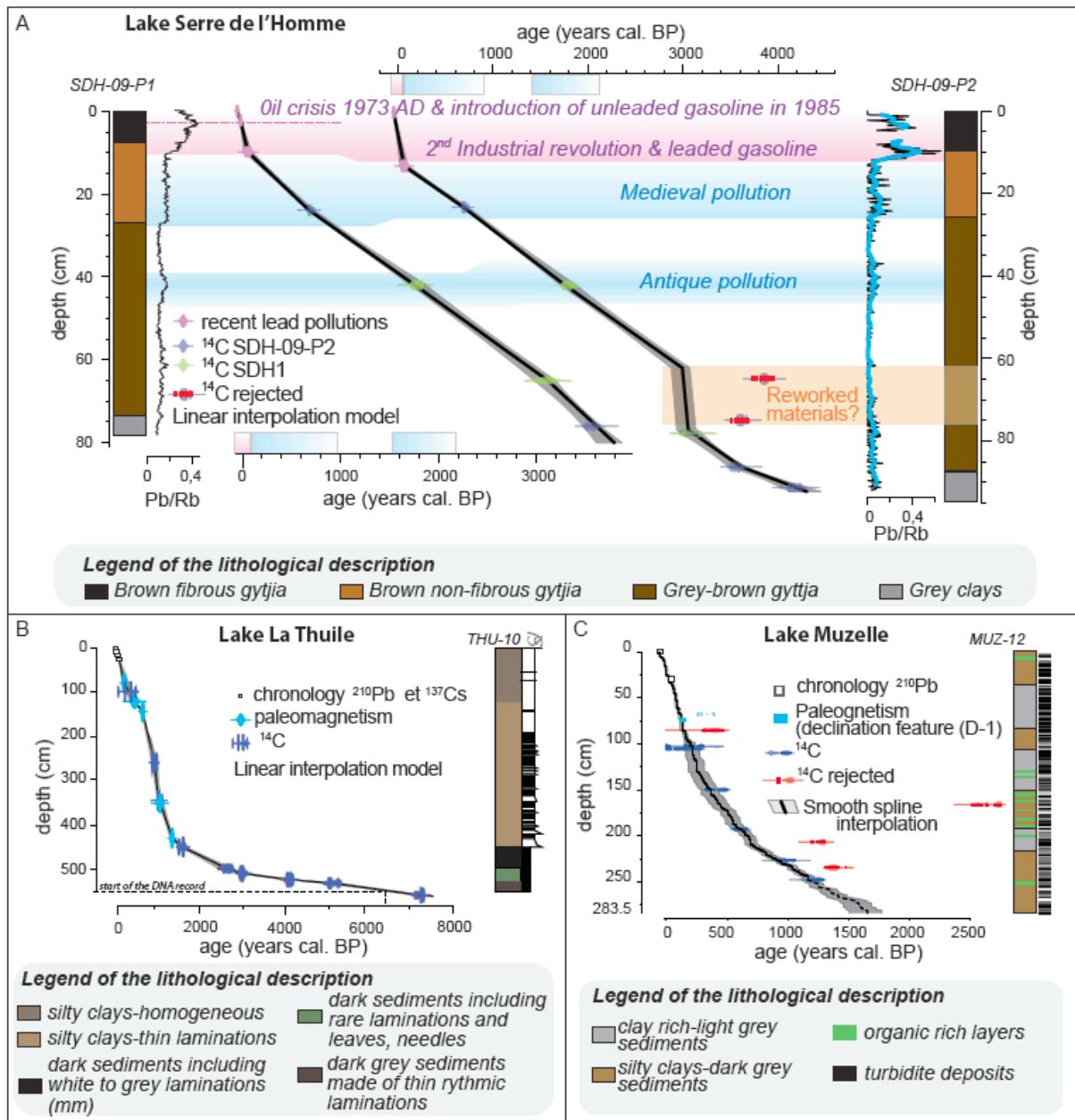
76  
 77 **Supplementary table 1. List of <sup>14</sup>C dates for Lake Serre de l'Homme.** Depth in grey and italic correspond to depth  
 78 determined by correlation. Samples in bold correspond to rejected dates.

	SDH 1		SDH-09-P2		SDH-09-P1		material dated	uncalibrated ages (BP) & uncertainty	Calibrated age ranges at 95% confidence intervals (cal. BP)
	top depth (cm)	bottom depth (cm)	top depth (cm)	bottom depth (cm)	top depth (cm)	bottom depth (cm)			
Poz-46475			23	24	24	25	Juniperus twig	740 +/-30	725-660
Poz-18880	33	34	<i>31</i>	<i>32</i>	32	33	bulk sediment	1385 +/-30	1345-1275
<b>Poz-46476</b>			<b>65</b>	<b>66</b>			<b>wood pieces (including a Brachyblast of P. cembra P.cembra and organic matter)</b>	<b>3565 +/-35</b>	<b>3725-3970</b>
<b>Poz-46477</b>			<b>75</b>	<b>76</b>			<b>matter</b>	<b>3375 +/-35</b>	<b>3510-3700</b>
Poz-18881	73	74	<i>78</i>	<i>79</i>	65	66	bulk sediment	2930 +/-35	2965-3175
Poz-35074			86		<i>76</i>		Conifer (Larix/Picea)	3320 +/-35	3465-3635
Poz-46478			91	92			pieces of wood and organic matter	3785 +/-35	4005-4290

79

80

81 The age-depth models built using the  $^{14}\text{C}$  dates and recent lead pollution markers are supported by  
82 older lead pollution phases detected by the XRF core scanner (Pb/Rb ratio). The most recent one  
83 starts around 900-950 cal. BP (11<sup>th</sup> century) and fits with the exploitation of two nearby mines  
84 (Faravel and L'Argentière-La Bessée) between the 10<sup>th</sup> and 13-14<sup>th</sup> centuries <sup>5</sup>. The other one  
85 corresponds to the Antique period (peak around 2100-2150 cal. BP, i.e. 150-200 BC). This  
86 pollution was also detected in a peat core (Fangeas) located in the neighbouring valley <sup>5</sup>. The  
87 origin, local vs regional/global, of this pollution could not be determined by the study by Py et al  
88 <sup>5</sup>. However, Roman-period pollution was also detected in several lakes and peats in French Alps  
89 <sup>6-8</sup> and Swiss Alps <sup>9-11</sup>, between 2500 and 1650 cal. BP, according to the sites.



90

91 **Supplementary figure 2. Age-depth models of the three lake sediment cores.** A) Age-depth model on cores SDH-  
 92 09-P1 and P2. B) Age-depth model on core THU-10. C) Age-depth model considering instantaneous deposits on core  
 93 MUZ-12. The lithological descriptions of each core are also presented.

94

## 95 1.2. Lake La Thuile

96 The lithology of the upper 549 cm of the core from Lake La Thuile is divided into five units, which  
 97 are described in detail in Bajard et al.<sup>12</sup> and summarized, here (Supplementary figure 2B). The two  
 98 upper units represent most of the sedimentation (0-190 cm and 190-450 cm). They are mainly  
 99 made of clays (10 to 40 %) and silts (40 to 80%). The lower unit is lighter and presents fine  
 100 laminations, while the upper one is darker and homogeneous. The organic matter content assessed

101 by the LOI at 550°C is less than 10% in these two units. Between 450 and 500 cm, sediments are  
102 very dark due to higher organic-matter content (20 to 30%). White to grey laminations are visible.  
103 From 500 to 530 cm, sediments are highly enriched in organic matter (around 50 to 60%) and  
104 contain well-preserved leaves. The lower 19 cm of the core was sampled for DNA analyses and  
105 is mostly characterised by very fine rhythmic laminations alternating between bio-precipitated  
106 carbonates (mostly rhombohedral calcite crystals) and diatoms.  
107 The age-depth model is based on nine <sup>14</sup>C dates and five chronological markers provided by the  
108 geomagnetic field secular variations (declination measured with three-axis 2-G enterprise  
109 cryogenic magnetometer of the CEREGE laboratory at Aix-Marseille University). The last  
110 hundred years are also constrained by short-lived radionuclide measurements (<sup>210</sup>Pb, <sup>137</sup>Cs, <sup>241</sup>Am).  
111 As for Lake Serre de l'Homme, the age-depth model was generated using the *R software* and the  
112 *R-code package 'Clam' version 2.2*<sup>4</sup>. The linear interpolation was selected (Supplementary figure  
113 2). More details about the sediment lithology and the age-depth model are available in Bajard et  
114 al.<sup>12</sup>.

115

### 116 **1.3. Lake Muzelle**

117 Sediments from Lake Muzelle are characterized by the presence of turbidite deposits all along the  
118 sediment core (Supplementary figure 2C). They are interpreted as flood deposits<sup>13</sup>. In the  
119 continuous sedimentation, three different facies were recognised: a light grey clay-rich facies, a  
120 dark grey silty clay facies and a facies enriched in organic matter. The two first facies alternate  
121 along the core to define seven units. The organic-rich facies mostly occurs bellow 140 cm depth  
122 and in the units made of the dark grey silty clay facies (Supplementary figure 2C). The darker  
123 facies is a little enriched in organic matter relative to the lighter one (4,4% vs 3,6% according to  
124 the LOI 550°C).

125 As turbidite deposits represent instantaneous deposits, they were not considered (time of  
126 deposition equal to zero) in the generation of the age-depth model (Supplementary figure 2C). Ten  
127 <sup>14</sup>C dates were performed, but four were rejected as too old probably due to reworked materials.  
128 One chronological marker provided by the geomagnetic field secular variations (also analysed at  
129 CEREGE laboratory) was also included in the age-depth modelling using the *R software* and the  
130 *R-code package 'Clam' version 2.2*<sup>4</sup>. The smooth spline interpolation was preferred for this lake  
131 (Supplementary figure 2C). More information about dating and sediment lithology are provided  
132 in Fouinat et al.<sup>13</sup>.

133

## 134 2. Filtering steps

### 135 2.1. Dealing with true and false presences

136 The summary of the numbers of reads from the high-throughput sequencing, and after the different  
137 filtering steps, is presented for plants in the supplementary figure 3. Several of these steps were  
138 used to remove potential false positives. Steps 1 to 8 (Supplementary figure 3), were realised using  
139 the OBITOOLS software (<http://www.grenoble.prabi.fr/trac/OBITools>)<sup>14</sup>, which allows, in  
140 particular, the removal of potential false positives due to PCR or sequencing errors. After these  
141 bioinformatic treatments, additional filtering steps (9 to 14) were applied to remove potential  
142 sporadic contaminations. In step 9, negative controls were used to detect false positives. Unique  
143 sequences (or Molecular Operational Taxonomic Units, MOTU) detected in at least one control  
144 (>5reads) only represent 15% of the total number of MOTU assigned to 95% of similarity with  
145 sequences in the reference database but represent 65 to 80% of the read numbers (whose 10 to  
146 16% are detected in the negative controls). On average, they mainly occur in the extraction controls  
147 for lakes Muzelle and La Thuile, and in PCR controls for Lake Serre de l'Homme (Supplementary  
148 table 2). In the filtering process, we only excluded the MOTU detected in high quantity in negative  
149 controls (in more than 5 controls with more than 10000 reads). These MOTU correspond to  
150 *Salicaceae sp.*, *Plantago sp.*, *Myriophyllum sp.*, *Asteraceae sp.* and *Lamiale sp.* for lakes Muzelle  
151 and La Thuile and *Betulaceae sp.* for Lake Serre de l'Homme (Supplementary table 2). Except for  
152 *Betulaceae sp.*, they also occur in a high number of samples with high read number and for some  
153 of them in several replicates. However, as they are detected in large quantities in the negative  
154 controls, we cannot be sure that their occurrences are not affected by contaminations. Moreover,  
155 the percentage of reads lost by the removal of these MOTU is higher in phases of lower total  
156 numbers of reads (Supplementary figure 4 and 5), which might be due to the preferential  
157 amplification of contaminants in samples containing less DNA. In Lake La Thuile, these MOTU  
158 are especially detected in very high quantity (representing up to 80% of the total read number)  
159 between 2600 and 3800 cal. BP (mostly *Lamiale sp.* and *Myriophyllum sp.*), which is a phase with  
160 a very high total number of reads but a low number of MOTU within the context of the whole  
161 dataset, i.e. without filtering (see blue area in Supplementary figure 4). Standard deviations of the  
162 total number of reads (between PCR from a common sample) are also very high, which shows a  
163 very stochastic amplification of the small number of MOTU detected in these samples and might  
164 indicate a contamination effect. The detection of a high number of DNA reads in this period is also  
165 suspicious because one extract dated to 3100 cal. BP (performed for another study) was quantified  
166 and gave a concentration lower than 0.05 ng/uL (i.e. under the detection limit of the Qubit

167 analysis). As presented and discussed in the manuscript, this phase is characterised by an  
168 accumulation of terrestrial plant macroremains (leaves, needles), which suggests a phase of litter  
169 erosion or direct fall of the macroremains in the lake. Humic substances present in the litter should  
170 have led to an acidification of the lake water. In addition, this hypothesis is supported by the  
171 absence of carbonate in the sediments, which only occurs during this period. Acidic conditions are  
172 not favourable to DNA preservation, which might explain the poor recording of DNA during this  
173 period. Moreover, DNA that might still eventually be present in this type of sediment is expected  
174 to be complexed with humic substances, which are not extracted by the method we used.

175

176 The next filtering step applied to limit potential false presences (step 11), was to remove MOTU  
177 detected in only one sample in each lake dataset (51 to 89 % are also detected in only one PCR).  
178 Then, MOTU only detected in one replicate per sample were discarded, unless they are detected  
179 in contiguous samples to consider the temporal autocorrelation which often affects ecological  
180 variables<sup>15</sup> (step 12). These two filtering steps allow the removal of MOTU considered doubtful  
181 (possibly rare taxa but also false presences). Again, the highest quantity of these MOTU is found  
182 between 2600 and 3800 cal. BP at Lake La Thuile (blue area in Supplementary figure 4). Many of  
183 the MOTU detected in low quantities in negative controls (less than 5 controls) were filtered out  
184 during these two filtering steps (21 and 26 over 49 for lakes Muzelle and La Thuile, respectively  
185 and 47 over 60 for Lake Serre de l'Homme).

186 The final step (13) of the filtering process common to all lakes was to remove taxa allochthonous  
187 in the Alps. In Lake Muzelle, six MOTU were assigned to *Grubbia Rosmarinifolia*, *Glycine max*,  
188 *Gaylussacia sp.*, *Styrax sp.*, *Cucumis sp.* and *Lactuca sativa*. The Grubbiaceae is a family of plants  
189 endemic to the Cape floristic region of South Africa. *Glycine max* (soy) comes from East Asia,  
190 *Gaylussacia sp.* (*Ericaceae* family) from America and the genus *Styrax sp.* from the Far East or  
191 the Mediterranean region. *Cucumis sp.* and *Lactuca sativa* are cultivated plants not supposed to  
192 grow at the altitude of the lake. In addition to some of these taxa, three other exotic taxa were  
193 removed from the Lake La Thuile dataset: *Actinidia*, *Axonopus* and *Musaceae*. *Axonopus* is a  
194 *Poaceae* from tropical and sub-tropical regions; *Actinidia* is the genus of kiwifruit and *Musaceae*  
195 the family of bananas.

196

197 In case of Lake La Thuile, a fourteenth step was applied to discard the last taxa that were detected  
198 in very high quantity only in the period when we think no or nearly no DNA was extracted  
199 (between 2600 and 3800 cal. BP). These taxa are *Pinus sp.*, *Populus sp.*, *Frangula sp.* and



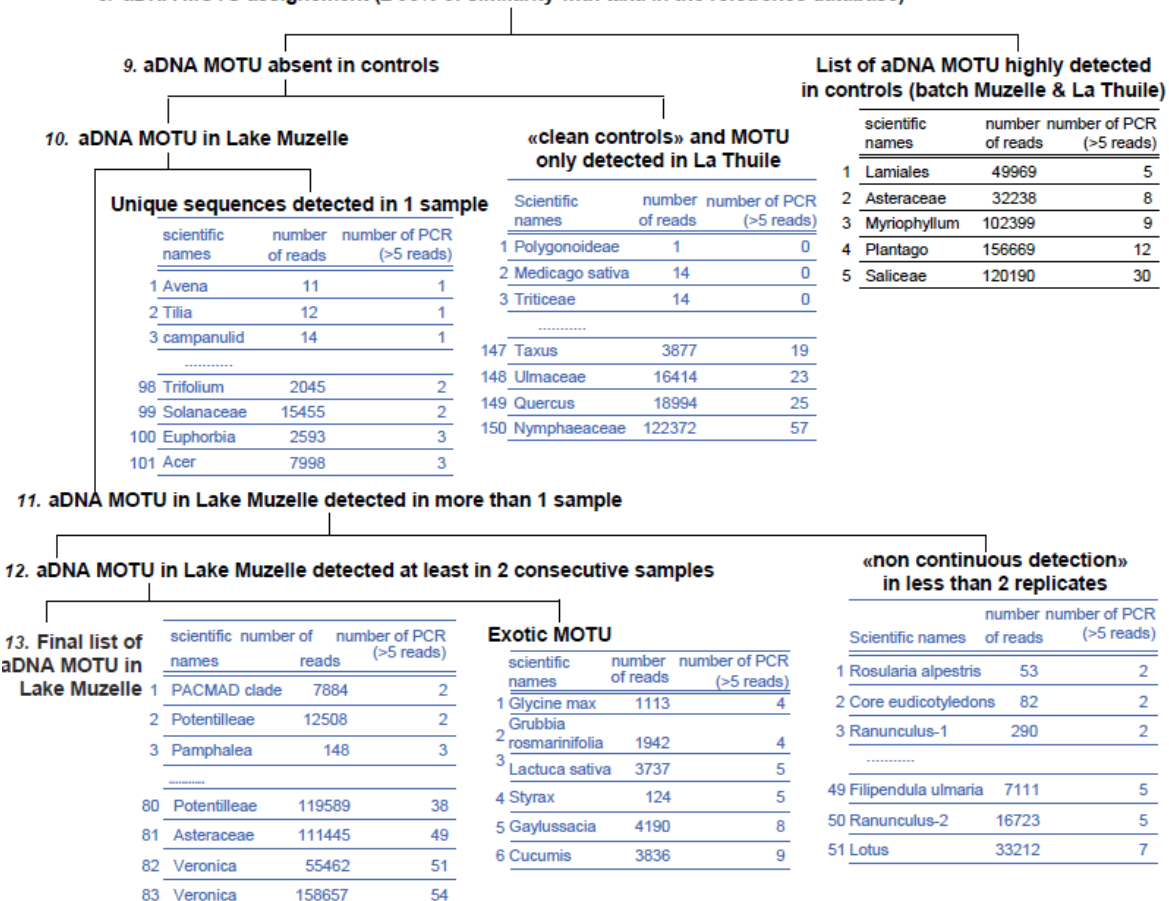
200 *Pooideae sp.*, which are not detected in the controls, and *Asteraceae sp.*, which is also detected in  
201 three extraction controls.

202

203 Even if they were sometimes detected in negative controls, we think that MOTU retained for the  
204 final datasets represent true signals because they possess temporal coherences, i.e. the occurrences  
205 of each plant are clustered in well-defined periods. Moreover, the temporal evolution of some of  
206 these MOTU is attested by independent methods. Specifically, pollen data (for La Thuile) and  
207 coprophilous fungi (for Muzelle) corroborated the detection of DNA from *Rumex sp.*, which was  
208 detected in 2 PCR controls (Figure 4 & 9). Likewise, for La Thuile, the DNA record of  
209 *Helianthemum nummularium* (detected in four different extraction controls with more than 5  
210 reads) is in agreement with the pollen record (Supplementary figure 8). For Lake Serre de  
211 l'Homme, the true presence of *Potamogeton sp.* (detected in three controls) and *Sparganium sp.*  
212 (detected in four controls) is supported by the increase of the organic matter content (LOI 550°C)  
213 and the decrease in the C/N ratio (i.e. increase of aquatic organic matter relative to terrestrial  
214 organic matter) (Figure 5). Moreover, the *Potamogeton sp.* mostly occurs at the same time as the  
215 Potamogetonaceae family, which is not detected in the controls (Figure 6). However, the record of  
216 the third aquatic plant detected in Lake Serre de l'Homme (*Myriophyllum sp.*) has to be considered  
217 with caution because it is mostly detected in only one or two replicates over eight (Figure 6) and  
218 is also detected in high quantities in negative controls (Supplementary table 2). Plant community  
219 composition and ecological preferences can also be used to support the occurrence of taxa. For  
220 instance, *Pinus sp.* (detected in 2 extraction controls) can be considered as accurate detections in  
221 the case of Lake Muzelle because they are contemporaneous with *Arctostaphylos uva-ursi*, a  
222 species associated with pinewood environments (Figure 8). It is also found in association with  
223 *Rhodoreae sp.* and *Vaccinium uliginosum* (Figure 8); two species characteristic of acid  
224 environments such as *Pinus sp.* likely to be found in this region. Moreover, pollen from *Pinus sp.*  
225 (*Pinus mugo* or *sylvestris*) occur during the Subatlantic period (covering the last 2500 years) in  
226 pollen diagrams from a peat area just below the lake<sup>16</sup>. By looking in detail at our datasets, we  
227 emphasise that distinguishing between true and false presences is not straightforward.

lake names	Muzelle (MUZ)	La Thuile (THU)	Muzelle (MUZ)	La Thuile (THU)	Serre de l'Homme (SDH)	
number of samples	30	50	30	50	41	
replicate number	4				8	
number of controls	64				56	
<b>Data filtering steps</b>	<b>No of reads</b>		<b>No of unique sequences</b>		<b>No of unique sequences</b>	
<b>1 Merging of paired-end reads</b>			-		-	
<b>2 Primer and tag identification</b>	12 401 846		-		-	
<b>3 Dereplication</b>	12 401 846		193 087		-	
<b>4 Filtering based on the sequence length</b>	12 355 683		191 587		-	
<b>5 Filtering of sequences without N</b>	12 110 708		161 773		-	
<b>6 Filtering based on the sequence occurrence (removal of sequences detected less than 100 times)</b>	11 478 425		3 224		-	
<b>7 Filtering on the status of each sequence in each PCR product (Removal of sequences more often «internal» than «head» or «singleton»)</b>	9 723 404		978		9 471 448 2 927	
<b>8 Assignment (percent identity ≥ 95% to database)</b>	7 405 225		396		8 700 614 438	
<b>9 Removal of MOTU highly detected in negative controls</b>	4 910 010		391		8 421 793 437	
<b>10 Removal of «clean controls» and split of datasets for MUZ and THU</b>	2 445 261	1 714 500	241	296	7 781 916	232
<b>11 Removal of MOTU detected in only 1 sample in each lake dataset</b>	2 197 260	1 617 191	140	180	6 813 710	49
<b>12 Removal of "non-continuous detections" in less than 2 replicates</b>	1 850 955	1 544 184	89	124	5 916 655	19 (7 aquatic and 12 terrestrial MOTU but 3 different aquatic taxa and 8 different terrestrial taxa)
<b>13 Removal of exotic MOTU</b>	1 836 110	1 475 651	83	112		
<b>14 Removal of other suspicious MOTU</b>		1 124 296		107 (10 aquatic MOTU probably corresponding to 10 different taxa)		

**8. aDNA MOTU assignment (≥ 95% of similarity with taxa in the reference database)**



228

229

230

231

**Supplementary figure 3. Information on aDNA plant datasets and flow chart of the filtering procedures.** Steps 1 to 8, were realised using the OBITOOLS software (<http://www.grenoble.prabi.fr/trac/OBITools>) (Boyer et al., 2016). The evolution of the number of reads and unique sequences at each step is presented, when it was calculated.

232 **Supplementary tables 2. List of contaminants in the sequencing run for plant DNA in lakes La Thuile and**  
 233 **Muzelle and then in Lake Serre de l'Homme.**

Lakes MUZELLE and La THUILE								
rank	scientific name	number of reads in samples	number of sample PCR >5reads	number of negative extraction controls	number of negative extraction controls (>5 reads)	number of negative PCR controls	number of negative PCR controls (>5 reads)	number of negative controls (>5 reads)
1	no rank	<i>campanulids</i>	234	15	6	1	0	1
2	tribe	<i>Poeae</i>	4181	7	0	0	12	1
3	no rank	<i>campanulids</i>	184	6	15	1	0	1
4	family	<i>Salicaceae</i>	126	8	23	1	0	1
5	family	<i>Salicaceae</i>	427	18	23	1	2	1
6	subclass	<i>asterids</i>	394	18	31	1	0	1
7	genus	<i>Trifolium</i>	75915	16	8	0	26	1
8	species	<i>Pentanema cernuum</i>	149	5	44	1	0	1
9	no rank	<i>campanulids</i>	270	2	59	1	0	1
10	species	<i>Vaccinium ovalifolium</i>	3204	14	0	0	72	1
11	order	<i>Asterales</i>	48	2	82	1	0	1
12	family	<i>Apiaceae</i>	29	2	92	1	0	1
13	genus	<i>Veronica</i>	58945	65	145	1	21	1
14	species	<i>Hedysarum hedysaroides</i>	26537	9	354	1	4	1
15	family	<i>Caprifoliaceae</i>	2825	3	517	1	3	1
16	subfamily	<i>Polygonoideae</i>	4	0	0	0	531	1
17	subfamily	<i>Pooideae</i>	7410	10	0	0	1268	1
18	family	<i>Betulaceae</i>	82758	35	16	0	1377	1
19	genus	<i>Equisetum</i>	3999	12	1	0	1542	1
20	species	<i>Bartsia alpina</i>	8414	11	1719	1	5	1
21	genus	<i>Gaylussacia</i>	4857	14	1	0	2008	1
22	species	<i>Pedicularis attollens</i>	197	1	3195	1	0	1
23	family	<i>Lamiaceae</i>	7374	8	3908	1	4	1
24	genus	<i>Geranium</i>	10258	14	5582	1	8	1
25	species	<i>Lomelosia brachiata</i>	188	3	6317	1	0	1
26	family	<i>Apiaceae</i>	110986	47	6300	1	58	1
27	family	<i>Ranunculaceae</i>	23947	7	8060	1	10	1
28	family	<i>Caprifoliaceae</i>	1603	3	10457	1	2	1
29	genus	<i>Caltha</i>	17527	16	14973	1	8	1
30	family	<i>Asteraceae</i>	17814	13	17140	1	12	1
31	species	<i>Medicago sativa</i>	27	0	1	0	20024	1
32	genus	<i>Veronica</i>	159619	66	22709	1	40	1
33	tribe	<i>Triticeae</i>	40	0	3	0	29205	1
34	genus	<i>Styrax</i>	130	5	23	2	1	2
35	family	<i>Apiaceae</i>	186	8	76	2	0	2
36	family	<i>Betulaceae</i>	1162	5	9	1	67	2
37	tribe	<i>Poeae</i>	92096	11	11	0	5754	2
38	genus	<i>Rumex</i>	11857	26	3	0	13126	2
39	family	<i>Betulaceae</i>	97	0	21635	1	12	2
40	subgenus	<i>Pinus</i>	184831	19	12	0	71048	2
41	species	<i>Lactuca sativa</i>	51820	16	112146	2	16	2
42	genus	<i>Alnus</i>	247474	114	42	2	49	3
43	genus	<i>Saxifraga</i>	47338	53	669	3	23	3
44	species	<i>Saxifraga oppositifolia</i>	24340	58	2875	3	13	3
45	genus	<i>Saxifraga</i>	47162	55	8620	3	20	3
46	species	<i>Saxifraga oppositifolia</i>	20986	61	10168	3	13	3
47	family	<i>Asteraceae</i>	196424	99	20762	3	54	3
48	family	<i>Betulaceae</i>	90	2	23218	2	55	3
49	species	<i>Athyrium vidalii</i>	62780	37	2525	1	28189	3
50	genus	<i>Cucumis</i>	4569	14	8196	4	1	4
51	family	<i>Betulaceae</i>	17393	14	5728	3	27542	4
52	species	<i>Helianthemum nummularium</i>	113917	56	33361	3	65	4
53	genus	<i>Picea</i>	31139	19	13	0	193530	4
54	order	<i>Lamiales</i>	180033	102	24757	3	25212	5
55	family	<i>Asteraceae</i>	302264	117	32136	6	102	8
56	genus	<i>Myriophyllum</i>	326449	129	91113	5	11286	9
57	genus	<i>Plantago</i>	599174	127	13722	4	142947	12
58	tribe	<i>Saliceae</i>	624830	247	110015	9	10175	30
total number of PCR		320	16	48	64			

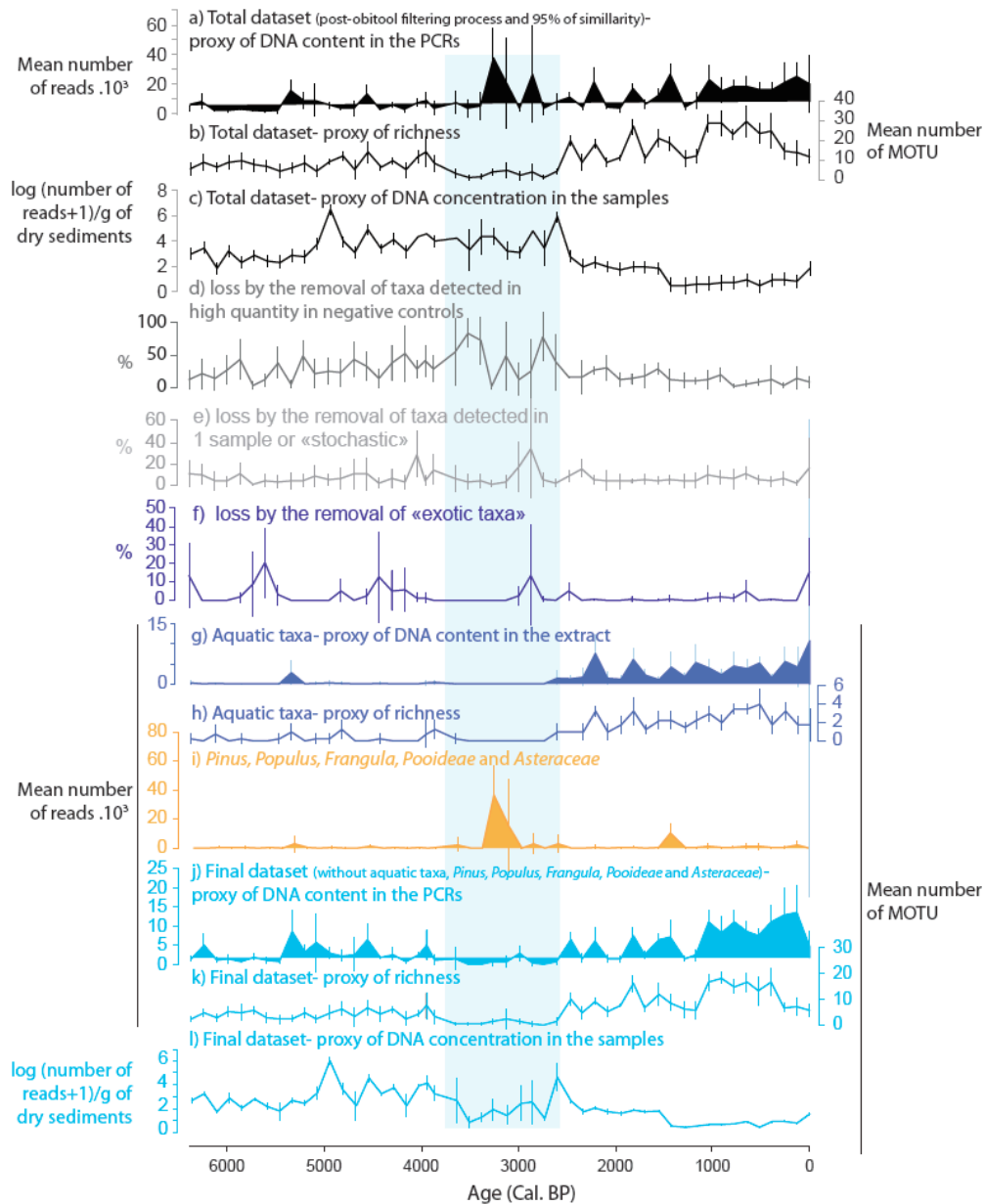
234

Lake SERRE de L'HOMME

rank	scientific name	number of reads in samples	number of sample PCR >5reads	number of negative extraction controls	number of negative extraction controls (>5 reads)	number of negative PCR controls (>5 reads)	number of negative PCR controls (>5 reads)	number of negative controls (>5 reads)
1	tribe <i>Poeae</i>	0	0	6	1	0	0	1
2	family <i>Apiaceae</i>	0	0	6	1	0	0	1
3	genus <i>Solanum</i>	0	0	6	1	0	0	1
4	tribe <i>Maleae</i>	1390	1	0	0	6	1	1
5	subfamily <i>Vaccinoideae</i>	0	0	0	0	8	1	1
6	species <i>Grubbia rosmarinifolia</i>	78	1	8	1	0	0	1
7	family <i>Salicaceae</i>	0	0	9	1	0	0	1
8	family <i>Solanaceae</i>	0	0	10	1	0	0	1
9	family <i>Apiaceae</i>	0	0	3	0	7	1	1
10	tribe <i>Poeae</i>	0	0	11	1	0	0	1
11	no rank <i>campanulids</i>	0	0	11	1	0	0	1
12	subclass <i>asterids</i>	41	1	11	1	0	0	1
13	genus <i>Empetrum</i>	0	0	0	0	12	1	1
14	order <i>Fagales</i>	45	2	8	1	4	0	1
15	subfamily <i>Solanoideae</i>	0	0	13	1	0	0	1
16	subfamily <i>Asteroideae</i>	1	0	17	1	0	0	1
17	no rank <i>BEP clade</i>	20729	4	0	0	28	1	1
18	genus <i>Caltha</i>	22228	4	25	1	4	0	1
19	no rank <i>Sanguisorbinae</i>	398296	7	30	1	3	0	1
20	genus <i>Huperzia</i>	0	0	0	0	36	1	1
21	genus <i>Huperzia</i>	0	0	0	0	44	1	1
22	genus <i>Huperzia</i>	0	0	0	0	44	1	1
23	genus <i>Rumex</i>	1488	2	0	0	50	1	1
24	genus <i>Gaylussacia</i>	35630	3	0	0	57	1	1
25	order <i>Asterales</i>	0	0	58	1	0	0	1
26	order <i>Ericales</i>	0	0	58	1	0	0	1
27	genus <i>Huperzia</i>	0	0	0	0	70	1	1
28	species <i>Vaccinium ovalifolium</i>	40659	3	0	0	123	1	1
29	tribe <i>Vaccinieae</i>	6368	2	0	0	159	1	1
30	genus <i>Isoetes</i>	24692	2	0	0	285	1	1
31	genus <i>Limonium</i>	0	0	454	1	0	0	1
32	genus <i>Solanum</i>	3	0	2280	1	0	0	1
33	tribe <i>Maleae</i>	3155	1	0	0	2363	1	1
34	genus <i>Sparganium</i>	1611392	35	30	0	2709	1	1
35	genus <i>Picea</i>	152851	3	4647	1	1	0	1
36	family <i>Asteraceae</i>	23608	1	4861	1	2	0	1
37	order <i>Asterales</i>	5	0	6283	1	1	0	1
38	species <i>Vaccinium uliginosum</i>	13	0	1	0	8332	1	1
39	genus <i>Theobroma</i>	5767	1	0	0	11300	1	1
40	genus <i>Actinidia</i>	74572	2	11895	1	2	0	1
41	genus <i>Avena</i>	2	0	0	0	14242	1	1
42	genus <i>Glycine</i>	7119	1	40250	1	2	0	1
43	genus <i>Bromus</i>	9	0	45687	1	1	0	1
44	no rank <i>Sanguisorbinae</i>	770	6	68980	1	1	0	1
45	subfamily <i>Pooideae</i>	191706	4	0	0	77720	1	1
46	genus <i>Caltha</i>	54	3	85525	1	0	0	1
47	order <i>Fagales</i>	0	0	8	1	18	1	2
48	tribe <i>Poeae</i>	243	2	13	1	16	1	2
49	tribe <i>Poeae</i>	12640	2	67	1	109	1	2
50	species <i>Filipendula ulmaria</i>	74367	3	16	1	829	1	2
51	genus <i>Empetrum</i>	9361	3	2	0	3153	2	2
52	species <i>Athyrium vidalii</i>	7543	4	1739	1	1658	1	2
53	species <i>Filipendula ulmaria</i>	141	3	2888	1	1090	1	2
54	order <i>Lamiales</i>	32992	3	4424	2	1	0	2
55	tribe <i>Saliceae</i>	174359	5	6865	1	871	1	2
56	tribe <i>Poeae</i>	29414	2	29261	1	23634	1	2
57	genus <i>Potamogeton</i>	1942111	34	2647	1	34	2	3
58	species <i>Athyrium vidalii</i>	58730	7	7460	1	8215	2	3
59	family <i>Apiaceae</i>	209904	7	11363	3	11013	1	4
60	genus <i>Myriophyllum</i>	961603	26	20851	1	111898	3	4
61	family <i>Betulaceae</i>	38738	7	7591	1	232492	4	5
total number of PCR		320		32		24		56

235

236



237

238

**Supplementary figure 4. Impact of the filtering process on the number of reads and of MOTU for Lake La**

239

**Thuile.** Curves a, b and c represent, respectively, the number of reads, the number of MOTU and the log-transformed

240

number of reads normalised by the dry weight of sediment (means and standard deviations) when no filtering is applied

241

on taxa assigned at 95 % of similarity. The curves d, e and f represent the loss percentages of DNA reads at three

242

different filtering steps: d) removal of MOTU detected in high quantity in controls, e) removal of MOTU detected in

243

only one sample or stochastically, f) removal of exotic MOTU. The curves g and h represent the distribution over time

244

of aquatic plants, in term of mean and standard deviation of the number of reads and of MOTU, respectively. The

245

curve i represent the stacking of five taxa remaining after the application of the thirteenth steps of filtering and

246

specifically detected during the period between 2600 and 3800 cal. BP (light blue area). They are removed in the

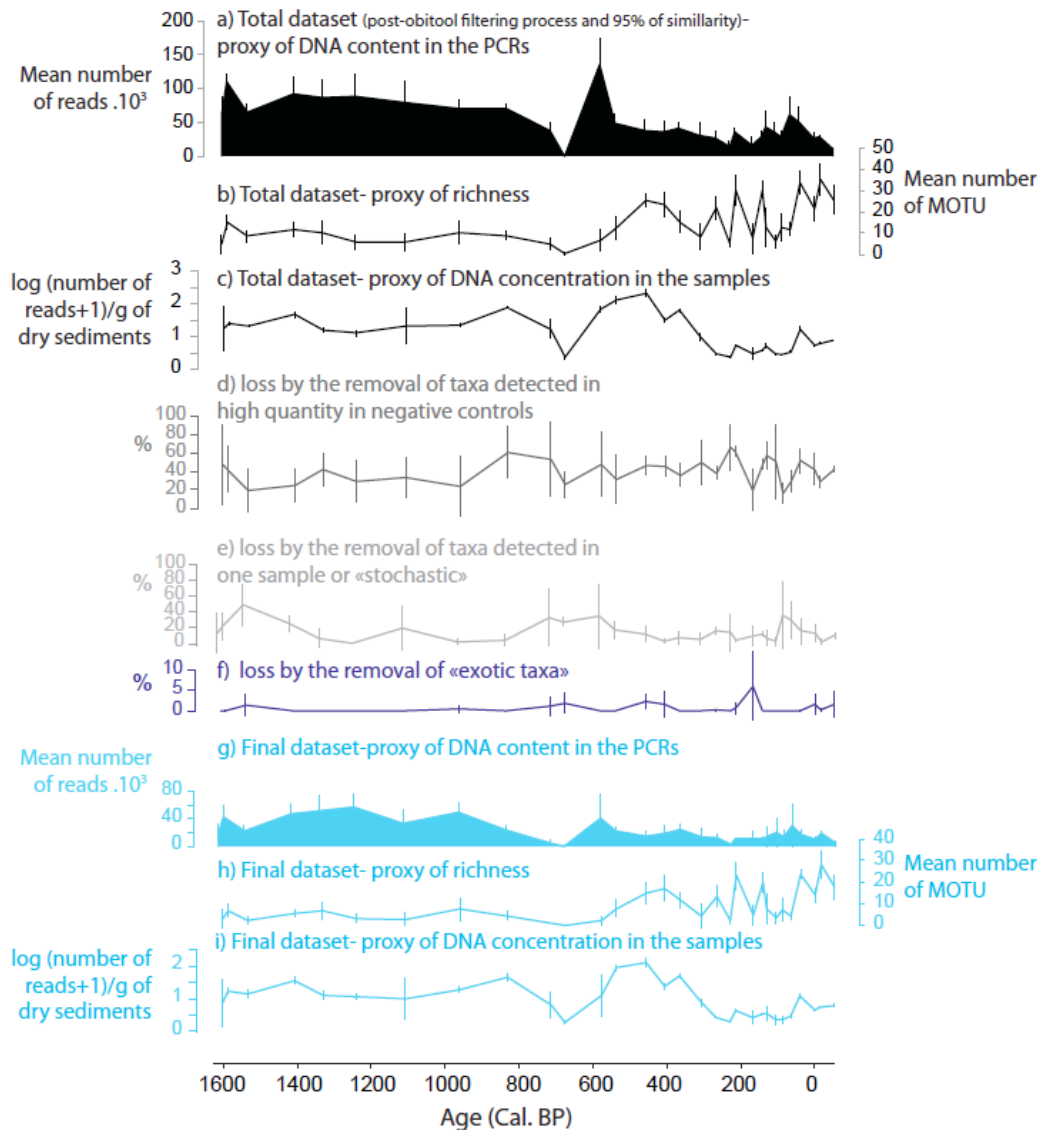
247

fourteenth step to obtain the final curves j, k and l (mean and standard deviation of the number of reads (j) and MOTU

248

(k) and of the log-transformed number of reads normalised by the dry weight of sediment (l)).

249



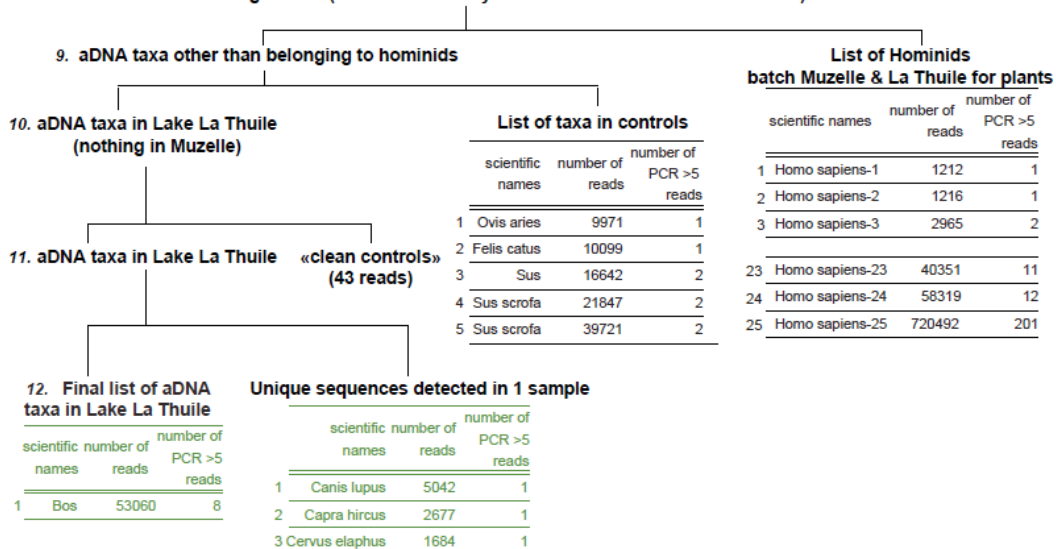
250  
 251 **Supplementary figure 5. Impact of the filtering process on the number of reads and of MOTU for Lake Muzelle.**  
 252 Curves a, b and c represent, respectively, the number of reads, the number of MOTU and the log-transformed number  
 253 of reads normalised by the dry weight of sediment (means and standard deviations) when no filtering is applied on  
 254 taxa assigned at 95 % of similarity. The curves d, e and f represent the loss percentages of DNA reads at three different  
 255 filtering steps: d) removal of MOTU detected in high quantity in controls, e) removal of MOTU detected in only one  
 256 sample or stochastically, f) removal of exotic MOTU. After the removal of these MOTU, the final curves g, h and i  
 257 are obtained (mean and standard deviation of the number of reads (g) and MOTU (h) and of the log-transformed  
 258 number of reads normalised by the dry weight of sediment (i)).

259  
 260 For mammals, the post-obitools filtering procedure starts, as for plants, with the removal of  
 261 sequences with a similarity  $<95\%$  to taxa in the reference database (step 8, Supplementary figure  
 262 6). However, the next step (9) consisted in the removal of human DNA sequences because they  
 263 mostly represent contaminations during sample processing. Whereas a human-specific blocking  
 264 oligonucleotide was applied, sequences from *Homo sapiens* (or assigned to lower taxonomic

265 levels, i.e. to *Homo*, *Homininae* and *Hominoidea*) are detected in high quantity (75 to 98% of read  
 266 numbers after the assignment to 95% of similarity). Then, the filtering process follows the same  
 267 procedure as for plants (Supplementary figure 6). However, we removed all taxa detected in  
 268 negative controls. These taxa are *Felis catus*, *Ovis aries*, *Sus sp.* and *Sus scrofa*. *Sus* and *Sus*  
 269 *scrofa* are common contaminants. They are mostly detected in samples from Lake La Thuile, and  
 270 detections in more than one replicate are clustered between 1000 and 800 cal. BP, i.e. when other  
 271 mammals (*Bos sp.* and *Ovis sp.*) are also detected (Figure 9). However, the second run performed  
 272 with a higher number of replicate to increase the detection probability (12 replicates) was not able  
 273 to confirm the presence of *Sus scrofa*, supporting the assumption of false presence. *Felis catus* was  
 274 never detected in samples and *Ovis aries* was detected in only two PCRs in Lake Muzelle and one  
 275 in Lake La Thuile.  
 276

lake names	Muzelle (MUZ)	La Thuile (THU)	Muzelle (MUZ)	La Thuile (THU)	Serre de l'Homme (SDH)
number of samples	30	50	30	50	40
replicate number	4				8
number of controls	64 but 56 identified				64 but 39 identified
<b>Data filtering steps</b>	<b>No of reads</b>		<b>No of unique sequences</b>		<b>No of unique sequences</b>
1 Merging of paired-end reads			-	8 815 609	-
2 Primer and tag identification	3 927 977		-	8 178 352	-
3 Dereplication	3 927 977		188 256	8 178 352	86 500
4 Filtering based on the sequence length	3 124 084		145 782	7 987 849	75 522
5 Filtering of sequences without N	2 687 190		55 004	7 985 409	74 574
Filtering based on the sequence occurrence (removal of sequences detected less than 100 times)	2 511 013		853	7 710 767	1 300
Filtering on the status of each sequence in each PCR product	1 940 128		319	6 917 247	279
6 Assignment (percent identity $\geq$ 95% to database)	1 322 537		34	5 518 002	40
7 Removal of <i>Homo sapiens</i> , <i>Homo</i> , <i>Homininae</i> , <i>Hominoidea</i>	327 649		9	131 507	2
8 Removal of MOTU detected in negative controls	62506		4	131 507	2
9 Removal of negative controls and split of dataset for MUZ and THU	0	62463	0	4	131 502
10 Removal of unique sequences detected in only 1 sample in each lake dataset	-	53060	-	1	131 345
11 Removal of stochastic detections in less than 2 replicates	-	53060	-	1	0

8. aDNA taxa assignment ( $\geq$  95% of similarity with taxa in the reference database)



277

278 **Supplementary figure 6. Information on aDNA mammal datasets and flow chart of the filtering steps.** Steps 1  
279 to 8, were realised using the OBITOOLS software (<http://www.grenoble.prabi.fr/trac/OBITools>) (Boyer et al., 2016).  
280 The evolution of the number of reads and unique sequences at each step is presented, when it was calculated. For Lake  
281 La Thuile, we only present the results of the filtering process from the first sequencing run. Another run of sequencing  
282 was performed with a higher number of PCR replicates (12) in order to increase the detection probability of mammals  
283 and attest the presence of cattle (only detected in one over four replicates in the first run). The second run improved  
284 the detection of cattle and also allowed to detect sheep (see manuscript).  
285

## 286 **2.2. Impact of the filtering procedure on the main results of the study**

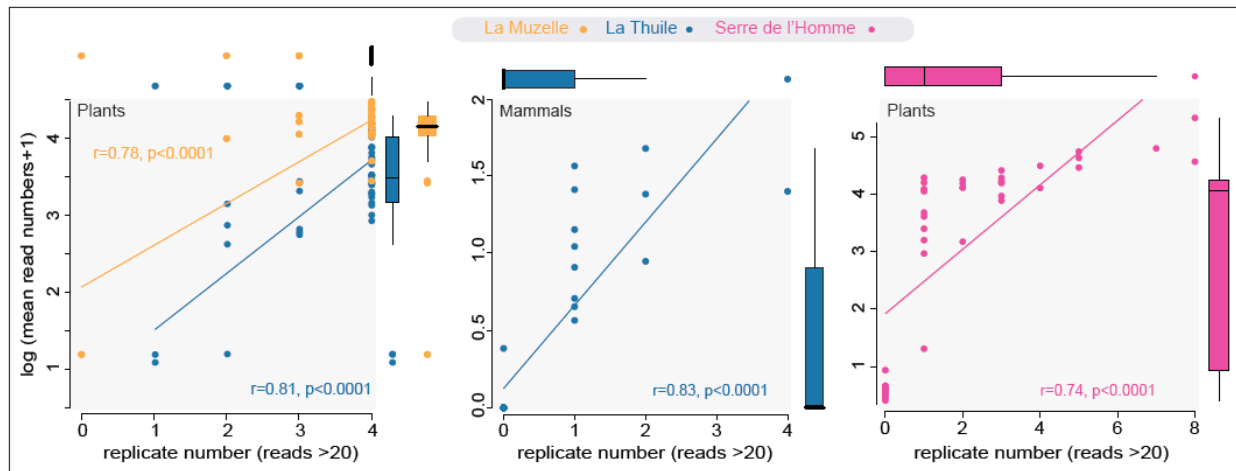
287 In order to assess the impact of the filtering steps (post-obitools treatment, from step 9 in  
288 supplementary figures 3) on the results of the study for terrestrial plants, the numbers of reads, of  
289 MOTU, and the log-transformed number of reads normalised by the dry weight of sediments  
290 (mean and standard deviation), are presented before and after the application of the filtering  
291 procedure for both lakes, La Thuile and Muzelle (Supplementary figures 4 and 5, respectively).  
292 The loss in percentages of DNA reads during the steps of the filtering process are also presented.  
293 The percentage of reads lost by the removal of MOTU considered as contaminants tends to be  
294 higher in phases in which lower total number of reads were detected (before the filtering step 9),  
295 except between 2600 and 3800 cal. BP at Lake La Thuile (blue area in the supplementary figure  
296 4). As previously stated, this trend probably reflects the preferential amplification of contaminants  
297 in poor DNA samples. This hypothesis is also valid for the phase between 2600 and 3800 cal. BP  
298 at Lake La Thuile, but as probably almost no aDNA fragments were extracted, the contaminants  
299 were “over amplified” during the PCR, which leads to the very high number of reads obtained  
300 before the application of the filtering procedure. The patterns of the number of reads in the final  
301 datasets are thus only accentuated relative to the patterns before the filtering, except between 2600  
302 and 3800 cal. BP at Lake La Thuile, when the highest numbers of DNA reads reach values close  
303 to zero after the filtering steps. Regarding the number of MOTU, the temporal patterns before and  
304 after the filtering are the same. The patterns are also retained (or slightly accentuated between  
305 2600 and 3800 cal. BP at Lake La Thuile) for the log-transformed number of reads normalised by  
306 the dry weight of sediments, i.e. for the proxy of the DNA concentration in the samples  
307 (Supplementary figures 4 and 5). Consequently, whether a filtering procedure is applied or not, it  
308 has no impact on the conclusions of our manuscript. If we apply a more stringent filtering, i.e.  
309 removing all the taxa detected in the negative controls, it does not change the patterns either.  
310  
311



### 312 3. Metabarcoding data and DNA quantity

313 The goal of DNA metabarcoding is to identify taxa present in environmental samples<sup>17</sup>. DNA  
314 metabarcoding analyses provide numbers of reads of the different taxa detected in a set of  
315 environmental samples. Usually, this number of reads is not considered as representative of a DNA  
316 quantity but only used to determine the presence/absence of taxa. To increase the detection  
317 probability and help detect the presence of false positives, multiple replicates can be used<sup>18,19</sup>. The  
318 number of positive replicates has also been proposed elsewhere as a proxy for the DNA quantity  
319 in a sample (e.g. in studies of lake sediment DNA<sup>20,21</sup> and environmental DNA<sup>19</sup>). This proxy was  
320 considered as a “more conservative interpretation more appropriate for aDNA” than the number  
321 of reads<sup>20</sup>. However, in a previous study on environmental DNA (plant DNA) from old terraces  
322 representing a chronosequence of crop abandonments (French Alps), the number of reads was also  
323 used as a quantitative variable<sup>22</sup>. In fact, they showed a negative relationship between the number  
324 of reads ( $\log(x+1)$ ) of a specific crop plant and the number of years since the abandonment of this  
325 crop. This result was interpreted as reflecting the DNA degradation in soils, and thus implicitly  
326 means the number of reads was considered as representing a DNA quantity present in the soil.  
327 They also showed correlations between the aboveground plant biomass and the abundance in DNA  
328 reads detected in the soil. Another study on environmental DNA from lake water also showed  
329 some correlations between fish biomass and the number of fish DNA reads<sup>23</sup>. Regarding the lake  
330 sediment DNA, a study comparing the number of positive replicates, the number of reads, pollen  
331 data and historical maps also highlighted the potential of the number of DNA reads as a “semi-  
332 quantitative” proxy, i.e. giving a magnitude of the DNA quantity in a sample compared to another  
333 one<sup>24</sup>. In the present study, we also propose that the number of reads can be used as a proxy for  
334 DNA quantity, to compare between samples (analysed in the same run of sequencing). Indeed, for  
335 plants at lakes La Thuile, Muzelle and Serre de l’Homme, we found a relationship between the  
336 log-transformed mean number of reads ( $\log(N \text{ reads}+1)$ ) and the number of replicates ( $r = 0.78$ ,  
337  $p < 0.0001$  for Muzelle;  $r = 0.81$ ,  $p < 0.0001$  for La Thuile,  $r = 0.74$ ,  $p < 0.0001$  for Serre de l’Homme;  
338 Supplementary figure 7). A significant positive correlation is also observed for mammals detected  
339 in Lake La Thuile ( $r = 0.83$ ,  $p < 0.0001$ ; Supplementary figure 7). However, for mammals at Lake  
340 La Thuile and plants at Lake Serre de l’Homme, we note a wide range of read numbers when DNA  
341 is detected in only one or two replicates. This might reflect the stochasticity of DNA amplification  
342 when the amount of DNA is very low. Given the high correlation coefficient between the number  
343 of positive replicates and the mean number of reads, we propose to use the mean number of reads

344 between a reasonable number of replicates, even if it is probably less robust than the number of  
 345 replicates and means cautions should be taken for the interpretations.  
 346  
 347



348  
 349 **Supplementary figure 7. Comparison between the means numbers of reads and the number of positive**  
 350 **replicates (>20 reads).** On the left, bi-plot for plants in lakes La Thuile (including aquatic and terrestrial plants, 50

351 samples) and La Muzelle (30 samples). In the middle, bi-plot for mammals in Lake La Thuile (33 samples). On the

352 right, bi-plot for plants in Lake Serre de l'Homme (including terrestrial and aquatic plants, 40 samples).

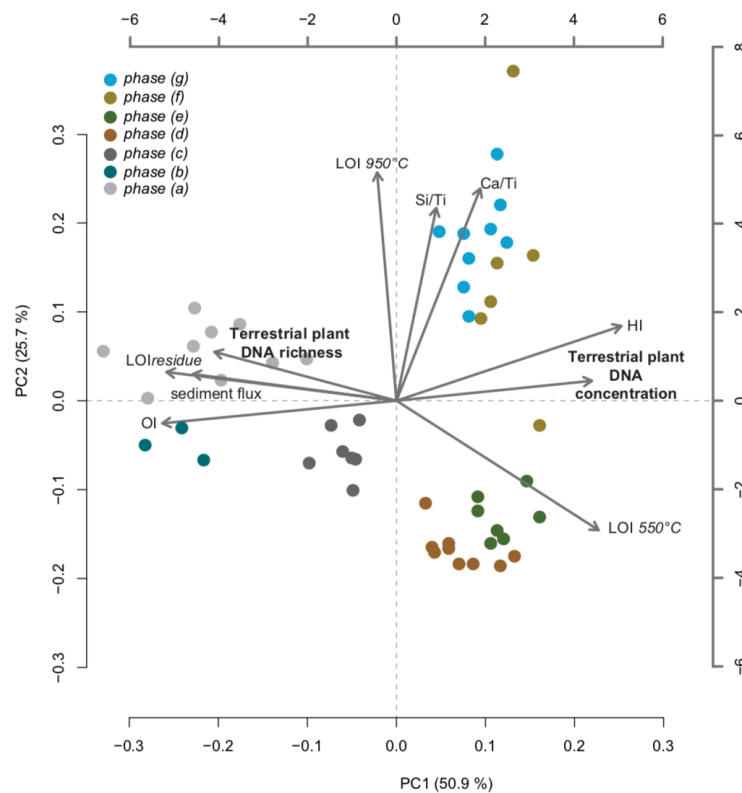
353

#### 354 4. Complementary analysis and data on Lake La Thuile

##### 355 4.1. PCA analysis of terrestrial plant DNA, sedimentological and geochemical data

356 In order to synthesise the results from the comparison of the terrestrial plant DNA concentration  
 357 and richness with the sedimentological and geochemical data, we perform a PCA analysis  
 358 (Supplementary Figure 8). For this purpose, we have to resample the XRF core scanner data (Si/Ti  
 359 and Ca/Ti used as proxies of the aquatic production) and interpolate the data from the Rock-Eval  
 360 Pyrolysis (Hydrogen and Oxygen Indexes used as proxies of a mixture between lacustrine and  
 361 litter organic matters and of organic matter from deep soil horizons, respectively). This is because  
 362 they were not measured at the same depths as the DNA. Despite the interpolation of some data,  
 363 the PCA analysis confirms our interpretations presented in the main text. A first end-member is  
 364 strongly correlated with the positive side of the first component. It includes the organic matter  
 365 (LOI 550°C) mostly derived from the litter (Hydrogen Index, HI and presence of leaves in the  
 366 sediments) and the DNA concentration. This end-member confirms the role of the biomass  
 367 production and of the source of eroded materials in the DNA concentration. The second end-  
 368 member is strongly correlated with the negative side of the first component. It represents the

369 detrital inputs (LOI residue and total sediment flux), i.e. the erosion and is also correlated with  
 370 terrestrial plant DNA richness. This correlation can be interpreted as follows; 1) as representing  
 371 the more efficient terrestrial plant DNA transfer triggered by, the higher erosion (increasing the  
 372 “catchment connectivity”) and/or, 2) as the result of the landscape opening which increases plant  
 373 diversity. We propose that these two processes occur because the richness in the pollen data also  
 374 increases; however, this increase is lower than in the DNA data. The last end-member is correlated  
 375 with the positive side of the second component. This end-member represents the aquatic  
 376 production (Si/Ti and Ca/Ti) and basic/neutral conditions (LOI 950°). The seven phases discussed  
 377 in the main text are well discriminated by the PCA analysis. Phase (b), characterised by a high OI  
 378 (Oxygen Index), provides evidence that deep soil horizons have poor DNA concentration, as the  
 379 DNA concentration and OI are negatively correlated. Phase (d), for which most samples are  
 380 characterised by a low DNA concentration, is negatively correlated with the second component  
 381 and positively correlated with the organic matter content. This pattern probably reflects the role of  
 382 acid conditions and/or of humic substances on the DNA preservation and/or our analytical  
 383 capacity.  
 384



385  
 386 **Supplementary figure 8. PCA analysis of the terrestrial plant DNA concentration and richness and the**  
 387 **sedimentological and geochemical data from Lake La Thuile sediments.** The first and second components  
 388 represent 50.9 % and 25.7 % of the variance. HI is the Hydrogen Index (mg HC/g TOC) and OI, the Oxygen Index

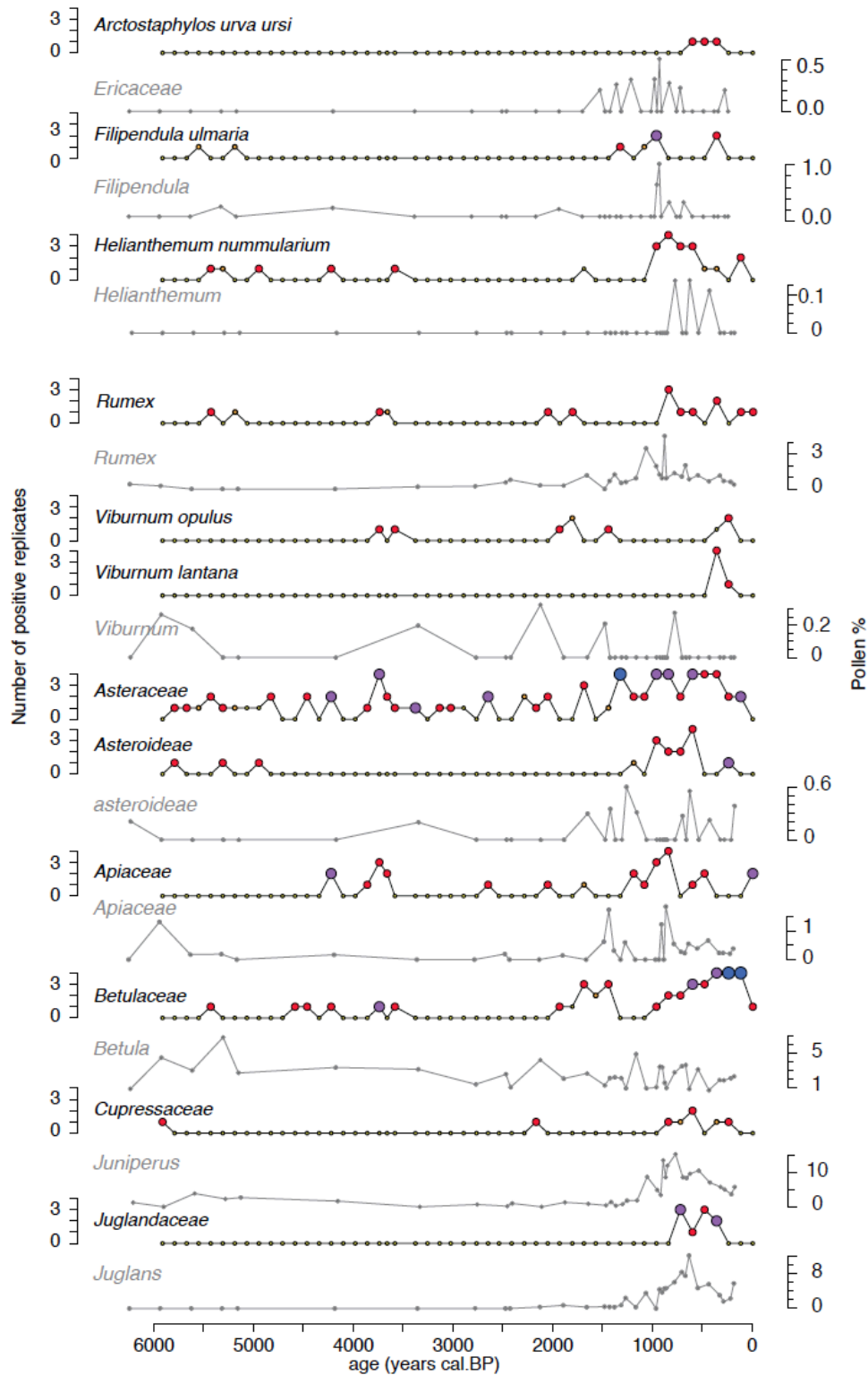
389 (mg O<sub>2</sub>/g TOC) of the organic matter. High HI values corresponds to a mixture between lacustrine and litter organic  
390 matters and high OI values show the presence of organic matter from deep soil horizons. Si/Ti and Ca/Ti are used as  
391 proxies of biogenic silica and bio-induced calcite, respectively. LOI residue and the total sediment flux are proxies of  
392 the erosion. LOI 550°C and LOI 950°C represent the contents in organic matter and carbonates, respectively. The  
393 samples from the different phases (a, b, c, d, e, f, g) used in the study (determined from the changes in the terrestrial  
394 plant DNA concentration) are presented in different colours.

395

#### 396 **4.2. Comparisons between DNA and pollen**

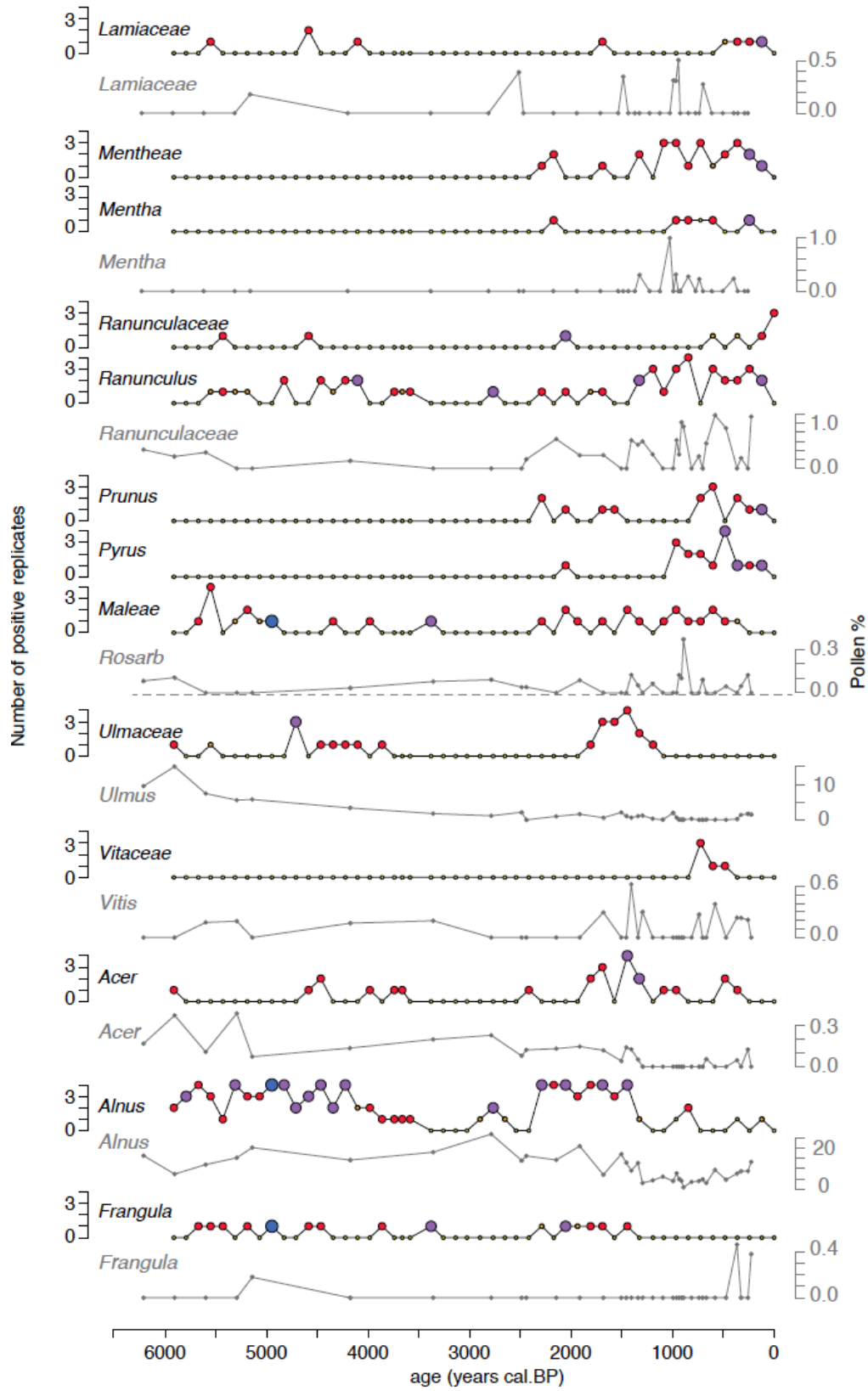
397

398



399

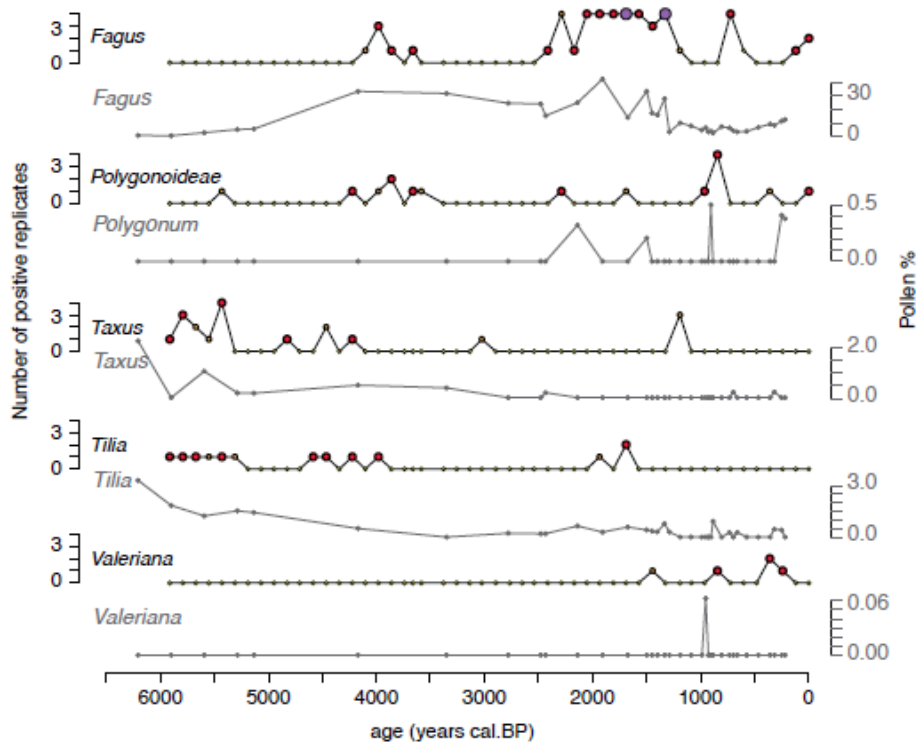
400 **Supplementary figures 9. Comparison between shared pollen (grey curves) and plant DNA taxa (black curves)**  
 401 **from Lake La Thuile sediments.** Taxa possibly shared, i.e. with different taxonomic resolution like *Juglans* (pollen)  
 402 and *Juglandaceae* (aDNA), are also presented.



403

404 **Supplementary figures 9 (next).**

405



406

407 **Supplementary figures 9 (end).**

408

409 **References**

410 1. Croudace, I. W., Rindby, A. & Rothwell, R. G. ITRAX: description and evaluation of a new  
 411 multi-function X-ray core scanner. *Geol. Soc. Lond. Spec. Publ.* **267**, 51–63 (2006).

412 2. Arnaud, F. *et al.* A 300 year history of lead contamination in northern French Alps  
 413 reconstructed from distant lake sediment records. *J Env. Monit* **6**, 448–456 (2004).

414 3. Weiss, D., Shotyk, W., Appleby, P. G., Kramers, J. D. & Cheburkin, A. K. Atmospheric Pb  
 415 Deposition since the Industrial Revolution Recorded by Five Swiss Peat Profiles: Enrichment  
 416 Factors, Fluxes, Isotopic Composition, and Sources. *Environ. Sci. Technol.* **33**, 1340–1352  
 417 (1999).

418 4. Blaauw, M. Methods and code for ‘classical’ age-modelling of radiocarbon sequences. *Quat.*  
 419 *Geochronol.* **5**, 512–518 (2010).

- 420 5. Py, V. *et al.* Interdisciplinary characterisation and environmental imprints of mining and  
421 forestry in the upper Durance valley (France) during the Holocene. *Quat. Int.* **353**, 74–97  
422 (2014).
- 423 6. Arnaud, F., Serralongue, J., Winiarski, T., Desmet, M. & Paterne, M. Pollution au plomb dans  
424 la Savoie antique (II–IIIe s. apr. J.-C.) en relation avec une installation métallurgique de la cité  
425 de Vienne. *Comptes Rendus Geosci.* **338**, 244–252 (2006).
- 426 7. Giguet-Covex, C. *et al.* Frequency and intensity of high-altitude floods over the last 3.5 ka in  
427 northwestern French Alps (Lake Anterne). *Quat. Res.* **77**, 12–22 (2012).
- 428 8. Guyard, H. *et al.* High-altitude varve records of abrupt environmental changes and mining  
429 activity over the last 4000 years in the Western French Alps (Lake Bramant, Grandes Rousses  
430 Massif). *Quat. Sci. Rev.* **26**, 2644–2660 (2007).
- 431 9. Shotyk, W. *et al.* History of Atmospheric Lead Deposition Since 12,370 <sup>14</sup>C yr BP from a Peat  
432 Bog, Jura Mountains, Switzerland. *Science* **281**, 1635 (1998).
- 433 10. Shotyk, W., Blaser, P., Grünig, A. & Cheburkin, A. K. A new approach for quantifying  
434 cumulative, anthropogenic, atmospheric lead deposition using peat cores from bogs: Pb in  
435 eight Swiss peat bog profiles. *Sci. Total Environ.* **249**, 281–295 (2000).
- 436 11. Thevenon, F., Guédron, S., Chiaradia, M., Loizeau, J.-L. & Poté, J. (Pre-) historic changes in  
437 natural and anthropogenic heavy metals deposition inferred from two contrasting Swiss Alpine  
438 lakes. *Quat. Sci. Rev.* **30**, 224–233 (2011).
- 439 12. Bajard, M. *et al.* Erosion record in Lake La Thuile sediments (Prealps, France): Evidence of  
440 montane landscape dynamics throughout the Holocene. *The Holocene* **26**, 350–364 (2016).
- 441 13. Fouinat, L. *et al.* One thousand seven hundred years of interaction between glacial activity and  
442 flood frequency in proglacial Lake Muzelle (western French Alps). *Quat. Res.* **87**, 407–422  
443 (2017).



- 444 14. Boyer, F. *et al.* OBITOOLS:aUNIX-inspired software package for DNAmetabarcoding. *Mol.*  
445 *Ecol. Resour.* **16**, 176–182 (2016).
- 446 15. Chen, W. & Ficetola, G. F. Conditionally autoregressive models improve occupancy analyses  
447 of autocorrelated data: An example with environmental DNA. *Mol. Ecol. Resour.* (2018).  
448 doi:10.1111/1755-0998.12949
- 449 16. Coûteaux, M. Fluctuations glaciaires de la fin du Würm dans les Alpes françaises, établies par  
450 des analyses polliniques. *Boreas* **12**, 35–56 (1983).
- 451 17. Taberlet, P., Coissac, E., Pompanon, F., Brochmann, C. & Willerslev, E. Towards next-  
452 generation biodiversity assessment using DNA metabarcoding: NEXT-GENERATION DNA  
453 METABARCODING. *Mol. Ecol.* **21**, 2045–2050 (2012).
- 454 18. Ficetola, G. F. *et al.* Replication levels, false presences and the estimation of the  
455 presence/absence from eDNA metabarcoding data. *Mol. Ecol. Resour.* **15**, 543–556 (2015).
- 456 19. Furlan, E. M., Gleeson, D., Hardy, C. M. & Duncan, R. P. A framework for estimating the  
457 sensitivity of eDNA surveys. *Mol. Ecol. Resour.* **16**, 641–654 (2016).
- 458 20. Alsos, I. G. *et al.* Sedimentary ancient DNA from Lake Skartjørna, Svalbard: Assessing the  
459 resilience of arctic flora to Holocene climate change. *The Holocene* **26**, 627–642 (2016).
- 460 21. Pansu, J. *et al.* Reconstructing long-term human impacts on plant communities: an ecological  
461 approach based on lake sediment DNA. *Mol. Ecol.* **24**, 1485–1498 (2015).
- 462 22. Yoccoz, N. G. *et al.* DNA from soil mirrors plant taxonomic and growth form diversity: DNA  
463 FROM SOIL MIRRORS PLANT DIVERSITY. *Mol. Ecol.* **21**, 3647–3655 (2012).
- 464 23. Evans, N. T. *et al.* Quantification of mesocosm fish and amphibian species diversity via  
465 environmental DNA metabarcoding. *Mol. Ecol. Resour.* **16**, 29–41 (2016).
- 466 24. Sjögren, P. *et al.* Lake sedimentary DNA accurately records 20<sup>th</sup> Century introductions of  
467 exotic conifers in Scotland. *New Phytol.* **213**, 929–941 (2017).
- 468

469

470

471